Ab Initio ECP/DFT Calculation and Interpretation of Carbon and Oxygen NMR Chemical Shift Tensors in Transition-Metal Carbonyl Complexes

Martin Kaupp,* Vladimir G. Malkin, Olga L. Malkina, and Dennis R. Salahub

Dedicated to Professor Paul von Ragué Schleyer on the occasion of his 65th birthday

Abstract: Carbon and oxygen NMR chemical shift tensors for Group 6 hexacarbonyl complexes $M(CO)_6$ (M = Cr, Mo, W) have been calculated by using a combination of quasirelativistic metal effective-core potentials and density-functional theory. Comparison with high-resolution solid-state shift tensors indicates excellent agreement between theory and experiment. The sensitivity of the shifts to the W–C distance in $W(CO)_6$ is discussed. A breakdown of the shielding tensor components into contributions from localized molecular orbitals allows the detailed interpretation of the trends on going down Group 6, and of differences to free CO. Group trends in the carbon shielding tensors are related largely to contributions from M–C σ-bonding orbitals. The presence of occupied metal $(n-1)$p and $(n-1)$d orbitals is partly responsible for the changes on going from free to metal-bound CO. The origin of the less pronounced trends in the oxygen shielding tensors is more complicated. The influence of scalar relativistic effects on the shift tensors has been studied for $W(CO)_6$ and is found to be relatively small, in spite of considerable changes in the W–C distance.

Keywords
density-functional theory · NMR chemical shifts · pseudopotentials · relativistic effects · transition-metal complexes

Introduction

The interpretation of NMR chemical shifts of carbonyl (and most other) ligands attached to transition metals is still an open question. The ab initio calculation of chemical shifts of compounds containing only main-group atoms up to the second long period has reached a remarkable state of accuracy, and detailed analyses of the factors contributing to these shifts have been made.[1] However, for heavy-element compounds in general, and for transition-metal complexes in particular, accurate calculations have not been possible owing to the difficulties of simultaneously treating electron correlation and relativistic effects.

Thus, discussion of the origin of chemical shifts in transition-metal complexes had to rely on rather approximate semi-empirical MO calculations and on crude qualitative arguments. As a result, some controversies over how to rationalize the observed trends have arisen over the years.[2] The carbon and oxygen shifts in the widely used carbonyl ligands are amongst the most prominent examples. Contradictory views on the mechanisms of these shifts, and the absence of reliable theoretical tools for their analysis, have led to considerable pessimism about whether a qualitative understanding will be reached.[2]

Very recently,[3] we have shown that accurate ligand chemical shifts in transition-metal compounds can be calculated by using a combination of sum-over-states density-functional perturbation theory (SOS-DFPT)[4] and quasirelativistic effective-core potentials (ECPs). Electron correlation is approximated by the exchange-correlation functional of the Kohn–Sham (KS) theory, at much lower computational cost[4] than needed for conventional correlated ab initio methods. Scalar relativistic effects due to the presence of a heavy transition metal are implicitly included by replacing the metal core electrons by a quasirelativistic ECP, while considering all electrons in the ligands of interest explicitly (additional heavy-atom spectator ligands may also be treated with ECPs).[3] It has been shown that even the ligand shifts of relatively large complexes may be calculated accurately by using this combination of methods.[3] The scalar relativistic contributions were found to be significant for 5d-metal oxo complexes.[5]

This new tool for the convenient and accurate calculation of the ligand chemical shifts in transition-metal complexes for the first time allows a thorough analysis of the origin of the observed trends. In addition to the isotropic shifts, the shift tensor elements are obtained from the calculations and may yield addi-

[*] M. Kaupp
Max-Planck-Institut für Festkörperforschung
Heisenbergstr. 1, D-70569 Stuttgart (Germany)
and
Institut für Theoretische Chemie, Universität Stuttgart
Pfaffenwaldring 55, D-70569 Stuttgart (Germany)
Telefax: Int. code + (711)689-1562
e-mail: kaupp@vsibm1.mpi-stuttgart.mpg.de
Vladimir G. Malkin
Institute of Inorganic Chemistry, Slovak Academy of Sciences
Dubravska Cesta 9, SK-84236 Bratislava (Slovakia)
O. L. Malkina
Computer Center, Faculty of Natural Sciences, Comenius University
Mlynska Dolina CH-1, SK-84215 Bratislava (Slovakia)
D. R. Salahub
Département de Chimie, Université de Montréal
C. P. 6128, Succ. centre-ville, Montréal, Québec H3C 3J7 (Canada)

0947-6539/96/0201-0024 $ 10.00+.25/0

tional information. One goal of the present article is to demonstrate the accuracy of the calculated tensor elements for some representative examples. As we use the SOS-DFPT with individual gauge for localized orbitals (IGLO),[6] a breakdown of both the individual tensor elements and of the isotropic shifts in terms of localized molecular orbital (LMO) contributions provides even more insight into the factors controlling the shifts. Alternatively, within the sum-over-states ansatz used,[4] the paramagnetic contributions to the shielding tensors may be analyzed in terms of dominant electronic excitations between canonical KS orbitals (by doing calculations with a common gauge origin). Together, these analytical tools aid in the development of a consistent picture of chemical shielding in metal carbonyl complexes. Only in a limited number of cases are shielding tensors of carbonyl complexes available from solid-state NMR spectroscopy.[7–10] These results have provided information, for example, on differences between bridging and terminal ligands[7, 8] and on dynamic processes in the solid state.[8, 9] In the present study, we have chosen the set of hexacarbonyl complexes $M(CO)_6$ (M = Cr, Mo, W) for detailed analysis, as high-resolution ^{13}C *and* ^{17}O shielding tensors for these species have been determined by Oldfield et al.[10] The study of these "normal" terminal carbonyl ligands will provide a standard against which to compare more unusual bonding arrangements in future work. Origins of periodic trends and of changes compared to free CO are investigated, and scalar relativistic contributions to the shift tensors are evaluated for $W(CO)_6$. Isotropic ^{13}C shieldings for these species have already been given as part of a larger data set used to validate our method.[3] To our knowledge this is the first study of NMR shielding tensors of transition-metal carbonyl complexes from first principles.[11]

Computational Methods

All calculations were carried out with a modified version of the LCGTO-MCP-DFT program deMon [12]. The SOS-DFPT approach used has been described in detail in ref. [4]. We use its LOC1 approximation [4]. The additional approximations involved in the combination of SOS-DFPT with quasirelativistic or nonrelativistic ECPs and the accuracy obtainable using this approach have been discussed in ref. [3]. The small-core energy-adjusted metal ECPs (and (8s7p6d)/[6s5p3d] valence basis sets) [13] are the same as in refs. [3,5] and have been transformed to nonlocal form [14] for technical reasons [15]. The transferability of this type of ab initio ECPs into DFT applications has been studied in detail and was found to be excellent [3,5,15,16]. Two types of all-electron basis sets, the IGLO-II and IGLO-III bases [6], have been compared for all carbon and oxygen atoms (i.e., in the present, more detailed study we do not employ the mixed ligand-basis approach proposed in ref. [3]).

Perdew and Wang's 1991 exchange-correlation potential [17] was used for the shift calculations. A "FINE" grid [4,12] was employed throughout this study. Auxiliary basis sets for the fit of exchange-correlation potential and charge-density were of the sizes 3,4 for the metals and 5,2 for carbon and oxygen (*n,m* designates *n* s functions and *m* spd shells). The IGLO procedure employed orbitals localized by the Foster/Boys scheme [18]. The C and O 1s orbitals were localized separately from the valence orbitals.

For a consistent evaluation of relativistic effects on $W(CO)_6$, all structures were optimized by using the same metal ECPs (for comparison both quasirelativistic and nonrelativistic for $W(CO)_6$ [13]) and valence bases as in the shift calculations but ECPs and DZP valence bases [19] (and 3,2 auxiliary sets) for C and O. The optimizations employed the Becke–Perdew exchange-correlation functional combination [20]. The quasirelativistic ECP/DFT optimizations yielded very good agreement of bond lengths (better than 0.02 Å) with the known solid-state structures of $Cr(CO)_6$ and $Mo(CO)_6$ (cf. Table 1). In the case of $W(CO)_6$, there is a significant difference (ca. 0.03 Å) between the gas-phase and the shorter solid-state W–C bond lengths. The calculated structure agrees well with the gas-phase data, that is, it gives W–C bond length that is longer (by ca. 0.04 Å) than that found in the solid-state structure. The influence of these structural changes on ligand chemical shielding is evaluated in the next sections. The nonrelativistic ECP/DFT optimization for $W(CO)_6$ gave a W–C bond length of 2.112 Å, another 0.04 Å longer than the quasirelativistic ECP results (Table 1), in good agreement with other nonrelativistic DFT calculations [21]. Throughout this paper we use the notation: method for chemical shift calculation//origin of structure, for example, QR//exp. indicates a quasirelativistic ECP calculation of the shift for the experimental structure.

Table 1. Calculated and experimental bond lengths (Å).

	CO	$Cr(CO)_6$	$Mo(CO)_6$	$W(CO)_6$
M-C				
exp. (gas-phase) [a]			2.063	2.058
exp. (solid-state) [b]		1.918	2.059	2.030
calc. (QR) [c]		1.910	2.064	2.073
calc. (NR) [d]				2.112
C–O				
exp. (gas-phase) [a]	1.128		1.145	1.148
exp. (solid-state) [b]		1.141	1.125	1.146
calc. (QR) [c]	1.140	1.154	1.152	1.154
calc. (NR) [d]				1.152

[a] From M. D. Harmony, V. W. Laurie, R. L. Kuczkowski, R. H. Schwendemann, D. A. Ramsay, F. J. Lovas, W. J. Lafferty, A. G. Maki, *J. Phys. Chem. Ref. Data* **1979**, *8*, 619 (CO), S. P. Arnesen, H. M. Seip, *Acta. Chim. Scand.* **1966**, *20*, 2711 ($Mo(CO)_6$, $W(CO)_6$). [b] From A. Jost, B. Rees, W. B. Yelon, *Acta Cryst. B* **1975**, *31*, 2649 ($Cr(CO)_6$); T. C. W. Mak, *Z. Krist.* **1984**, *166*, 277 ($Mo(CO)_6$); F. Heiermann, H. Schmidt, K. Peters, D. Thiery, *Z. Krist.* **1991**, *198*, 123 ($W(CO)_6$). [c] Quasirelativistic metal ECP. [d] Nonrelativistic metal ECP.

The reference compounds, namely, TMS (for ^{13}C shifts) and H_2O (for ^{17}O shifts), have been optimized at the same computational levels. The absolute ^{13}C shielding of TMS is calculated as 187.3 ppm at the basis II and as 184.0 ppm at the basis III level. The ^{17}O shielding of the water molecule is 300.3 ppm with basis II and 320.0 ppm with basis III.

Results and Discussion

A. Carbon Shift Tensors: In the upper half of Table 2, experimental and calculated (both with IGLO-II and IGLO-III bases) ^{13}C shift tensors are compared for free CO and for the hexacarbonyl complexes. The results for the isotropic shifts are also shown in Figure 1 (top). The calculated isotropic shift (δ_{av}) for free CO is approximately 12 ppm too low at the basis II level and approximately 9 ppm too low at the basis III level. Most correlated ab initio methods also give ^{13}C shifts that are somewhat too low, whereas coupled Hartree–Fock methods give values that are too large.[6, 22, 23]

Better agreement than for free CO is found for $Cr(CO)_6$ and $Mo(CO)_6$, where the IGLO-II and IGLO-III basis set results for the isotropic shift (δ_{av}) bracket the experimental values; the larger (IGLO-III) basis yields a slightly larger shift (Table 2). With the DFT-optimized W–C bond length, the smaller IGLO-II basis already exaggerates the value for $W(CO)_6$ by about 3 ppm, and the difference increases to around 11 ppm with the larger basis. The resulting deviation of calculated from experimental trends in the isotropic ^{13}C shifts is shown clearly in Figure 1 (top). With the shorter W–C bond length from the experimental solid-state structure, the shift decreases, and the periodic trend is reproduced much more closely (dashed lines in Fig. 1 top). The neglect of spin–orbit coupling in our calculations might also slightly influence the computed trends,[3] and we have not accounted for ro-vibrational or environmental corrections.

The trend towards increased shielding on going down the chromium triad is reproduced well, when the shorter W–C bond length of 2.030 Å (Table 1) is used (Fig. 1 top). As Gleeson and Vaughan[8] already observed, the increase in shielding arises largely from a corresponding decrease in the perpendicular shift tensor elements δ_{11} and δ_{22} (see below). The fact that coordination of CO to a Group 6 metal center leads to deshielding (again due to δ_{11} and δ_{22}) is also well described by the calculations.

The "experimental" ^{13}C shift-tensor elements for free CO given in Table 2 are those estimated by Gleeson and Vaughan[8]

Table 2. Comparison of calculated and experimental carbon and oxygen chemical shift tensors (ppm) for Group 6 hexacarbonyl complexes [a].

	CO			$Cr(CO)_6$			$Mo(CO)_6$			$W(CO)_6$				
	exp.	III [b]	II [c]	exp. [d]	III [b]	II [c]	exp. [d]	III [b]	II [c]	exp. [d]	QR//QR [j] III [b]	QR//QR [j] II [c]	QR//exp. [k] III [b]	QR//exp. [k] II [c]
C														
δ_{11}	(316 [e])	312	306	369	362	350	338	350	339	326	345	333	340	328
δ_{22}	(316 [e])	312	306	335	362	350	332	350	339	319	345	333	340	328
δ_{33}	(−90 [e])	−89	−86	−69	−76	−74	−65	−82	−81	−70	−81	−81	−83	−83
δ_{av}	186 [f]	178	175	212	216	208	202	206	199	192	202	195	199	191
$\delta_{\parallel}-\delta_{\perp}$	−406 (30) [g]	−401	−391	−421	−437	−423	−400	−432	−420	−393	−426	−414	−422	−411
O														
δ_{11}		602	576	651	633	605	621	614	577	603	597	560	580	550
δ_{22}		602	576	615	633	605	592	614	577	572	597	560	580	550
δ_{33}		−91	−115	−58	−39	−58	−43	−40	−64	−31	−33	−59	−32	−51
δ_{av}	386 [h]	371	346	403	408	384	400	396	364	384	387	354	376	350
$\delta_{\parallel}-\delta_{\perp}$	−653 [i]	−693	−691	−691	−670	−663	−650	−693	−642	−619	−630	−618	−612	−601

[a] Shifts referenced to TMS for carbon and to H_2O^{vap} for oxygen, with positive sign/more deshielded convention. Experimental ^{17}O data were converted by adding the experimental gas/liquid shift (+36 ppm) of water (cf. ref. [30]). [b] IGLO-III basis. [c] IGLO-II basis. [d] Ref. [10]. [e] Estimate [8] for motionally "unaveraged" free CO, see text. [f] Gas-phase data from ref. [26]. [g] See ref. [24]. [h] Ref. [30]. [i] W. H. Flygare, *Chem. Rev.* **1974**, *74*, 653. [j] At quasirelativistically optimized structure (cf. Table 1). [k] At experimental solid-state structure (cf. Table 1).

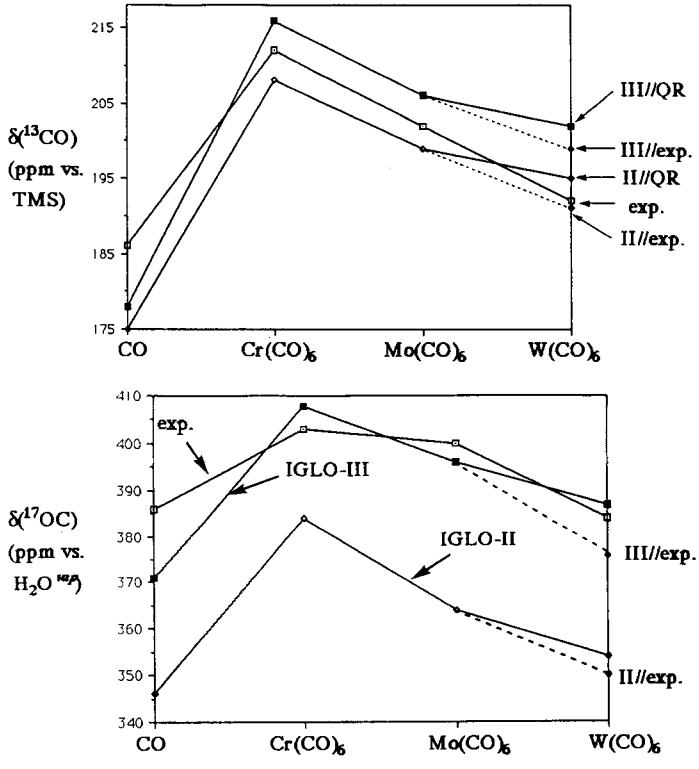

Fig. 1. Comparison of calculated and experimental isotropic NMR chemical shifts. Top: ^{13}C shifts. Bottom: ^{17}O shifts. See Table 2 for numerical data. Quasirelativistic ECP results; dashed lines refer to results obtained with the experimental solid-state W–C bond length (Table 1) of $W(CO)_6$.

from a "motionally unaveraged" anisotropy ($\delta_{\perp}-\delta_{\parallel}$) of 406(30) ppm given by Gibson et al.[24] In view of the experimental uncertainties, the agreement between these best estimates for free CO and our calculations is reasonable.

To compare experimental and computational results for the tensor components of the metal complexes, the measured δ_{11} and δ_{22} elements should be averaged ($\delta_{\perp} = (\delta_{11} + \delta_{22})/2$). The slight deviations from axial symmetry in the solid state have been ascribed to the reduced local symmetry in the crystal,[10] whereas the two values are identical within numerical error for our molecular calculations on perfect octahedral structures. The calculated $\delta_{\perp}$ for the metal complexes are slightly too large. Augmentation of the basis set increases them and thus also the differences to experiment. In contrast, the $\delta_{\parallel}$ (δ_{33}) elements are calculated to be somewhat too negative and are relatively insensitive to the basis set level (consistent with their diamagnetic character). The good agreement between theory and experiment for the isotropic shift of $Mo(CO)_6$ and $W(CO)_6$ is thus partly due to error compensation. Calculated shift anisotropies ($\delta_{\parallel}-\delta_{\perp}$) are therefore somewhat too negative. It should be noted, however, that the experimental error bars in the individual tensor elements and shift anisotropies are larger (estimated to be ca. 5–10 ppm[10]) than for isotropic shifts in solution. Thus, the computational results are either within or only slightly outside the experimental uncertainty margins. Moreover, part of the differences may be due to matrix effects contained in the solid-state data. Thus, the present results show that not only isotropic shifts, but also individual ^{13}C shift-tensor elements in these carbonyl complexes can be calculated accurately with our ECP/DFT approach, even if larger basis sets may lead to still slightly larger values.

B. Oxygen Shielding Tensors: Calculated isotropic ^{17}O shifts δ_{av} (see bottom halves of Table 2 and Fig. 1) are in good agreement with experiment at the basis III level (the largest deviation is ca. 15 ppm for free CO). The basis II results are somewhat (ca. 25–35 ppm) too low. There is less variation of the calculated isotropic shifts between the different complexes (compared to the carbon shifts and given the larger oxygen shift range) and free CO (a very small decrease from Cr to W), in agreement with experimental observation.

The $\delta_{\perp}$ (δ_{11} and δ_{22}) tensor elements exhibit somewhat larger variations, whereas $\delta_{\parallel}$ (δ_{33}) changes less from compound to compound. Agreement between calculation and experiment for the individual tensor elements is comparable to those for the isotropic shifts, that is, theory gives very good results at the basis III level, and values that are somewhat too low at the basis II level. Slightly larger deviations pertain to δ_{33} for $Cr(CO)_6$ with basis III. This obscures the experimentally observed[10] slight decrease of this tensor element from $Cr(CO)_6$ to $W(CO)_6$. As pointed out above for the carbon shielding tensors, the differences between the experimental δ_{11} and δ_{22} have been attributed to reduced symmetry in the crystal.[10]

0947-6539/96/0201-0026 $ 10.00+.25/0 Chem. Eur. J. 1996, 2, No. 1

C. Scalar Relativistic Contributions for $W(CO)_6$: Scalar relativistic effects, which may be evaluated by comparing results obtained with quasirelativistic and with nonrelativistic ECPs,[5] have been found to be important for the ^{17}O shifts in high-valent 5d-metal oxo complexes.[5] It is thus of interest to investigate the importance of these contributions for the present d^6 carbonyl species, particularly for the tungsten complex. In Table 3, both the influence of relativistic changes in the bond length, and direct electronic influences on the shift tensor of $W(CO)_6$ are evaluated. The relativistic bond length contraction leads, for example, to a reduction of approximately 2 ppm in $\delta_{av}(^{13}C)$ (cf. NR//QR vs. NR//NR columns), and the direct relativistic change of electronic structure contributes another -3 ppm to $\delta_{av}(^{13}C)$ (cf. QR//QR vs. NR//QR columns).

Table 3. Scalar relativistic effects on the chemical shift tensors (ppm) of $W(CO)_6$ [a].

	QR//QR [b]	NR//QR [c]	NR//NR [d]
C			
δ_{11}	344	349	351
δ_{22}	344	349	351
δ_{33}	− 82	− 84	− 83
δ_{av}	202	− 205	− 207
$\delta_{\parallel}-\delta_{\perp}$	− 426	− 433	− 434
O			
δ_{11}	597	612	617
δ_{22}	597	612	617
δ_{33}	− 33	− 41	− 42
δ_{av}	387	394	397
$\delta_{\parallel}-\delta_{\perp}$	− 630	− 653	− 659

[a] Shifts referenced to TMS for Carbon and to H_2O^{vap} for oxygen, with positive sign/more deshielded convention. IGLO-III basis on C and O. [b] Quasirelativistic ECP in shift calculation and in structure optimization. [c] Nonrelativistic ECP shift calculation at quasirelativistically optimized structure. [d] Nonrelativistic ECP in shift calculation and in structure optimization.

The scalar relativistic effects are surprisingly small in view of the significant (0.04 Å) relativistic contraction of the W–C bond (see Table 1). The overall changes remain below 7 ppm for ^{13}C shift tensor elements and below about 20 ppm for ^{17}O shift tensor elements. This may be compared to scalar relativistic contributions of more than 160 ppm to the ^{17}O shift in WO_4^{2-}.[5] Of course, the oxygen atoms are further removed from the metal center in the present case, so the oxygen shifts are not directly comparable.

D. Correlations between Shielding Tensors and Orbital Energy Differences: Within the present sum-over-states approach,[4] the paramagnetic contributions to the shielding tensor elements, $\sigma^p_{N,uv}$, are given by Equation (1). Thus, the orbital energy differences between occupied and virtual KS orbitals ($\varepsilon_k-\varepsilon_a$) are amongst the most important factors determining the magnitude of the contribution from a given excitation $k \rightarrow a$ (assuming that the corrections $\Delta E^{xc}_{k\rightarrow a}$ are small, i.e., starting from an uncoupled KS approach). One might therefore expect the energetically lowest-lying, magnetically allowed transitions $\psi_k \rightarrow \psi_a$ to largely control the paramagnetic shielding. For the Group 6 hexacarbonyl complexes (Table 4) this would be the $2t_{2g} \rightarrow 2e^*_g$, $2t_{2g} \rightarrow 3t^*_{2g}$, and $2t_{2g} \rightarrow 2t^*_{1g}$ transitions, followed at larger energies by $2t_{1u} \rightarrow 3t^*_{1u}$ and $2t_{1u} \rightarrow 2t^*_{2u}$. However, analysis of the SOS expression in terms of canonical KS orbitals (obtained from a separate calculation with a common gauge origin on the nucleus of interest, or alternatively at the metal nucleus to conserve the symmetry selection rules) indicates that a considerable number of different "excitations" over a large range of $\varepsilon_k-\varepsilon_a$ contribute significantly to the paramagnetic terms in the hexacarbonyl complexes. The largest overall contributions may be grouped into excitations out of mainly C–M σ-bonding ($1a_{1g}$, $1e_g$, $1t_{1u}$), C≡O bonding ($1t_{1g}$, $2t_{1u}$), and metal d-like ($2t_{2g}$) MOs, whereas the virtual orbitals involved are the ones appropriate by symmetry from the C≡O antibonding manifold ($3t^*_{1u}$, $2t^*_{2u}$, $3t^*_{2g}$, $2t^*_{1g}$). We should note here that the periodic trends of the ligand shielding and the shielding differences between free and metal-bound CO are reproduced reasonably well even with a common gauge origin.

$$\sigma^p_{N,uv} = -\frac{2}{c^2}\sum_k^{occ}\sum_a^{virt}\frac{\langle\psi_k|L_v|\psi_a\rangle\langle\psi_a|L_{N,u}r_N^{-3}|\psi_k\rangle}{\varepsilon_k-\varepsilon_a-\Delta E^{xc}_{k\rightarrow a}} \quad (1)$$

It is clear that compared to free CO the carbonyl complexes exhibit a larger number of possible low-energy excitations. However, simple explanations for the observed trends in terms of just a few individual orbital combinations do not emerge from the MO analysis. In particular, some contributions to

Table 4. Kohn–Sham orbital energies (a.u.) [a].

Symmetry	$Cr(CO)_6$	Symmetry	$Mo(CO)_6$	$W(CO)_6$ QR//QR [b]	$W(CO)_6$ NR//NR [c]
virtual MOs					
$4t^*_{1u}$	+ 0.005	$2e^*_g$	+ 0.007	+ 0.022	+ 0.014
$2a^*_{1g}$	− 0.026	$4t^*_{1u}$	+ 0.005	+ 0.007	+ 0.005
$2t^*_{1g}$	− 0.028	$3t^*_{2g}$	− 0.018	− 0.002	− 0.010
$2e^*_g$	− 0.034	$2a^*_{1g}$	− 0.022	− 0.025	− 0.022
$3t^*_{2g}$	− 0.057	$2t^*_{1g}$	− 0.044	− 0.048	− 0.044
$2t^*_{2u}$	− 0.074	$2t^*_{2u}$	− 0.082	− 0.086	− 0.079
$3t^*_{1u}$	− 0.090	$3t^*_{1u}$	− 0.103	− 0.107	− 0.101
occupied MOs					
$2t_{2g}$	− 0.238	$2t_{2g}$	− 0.237	− 0.237	− 0.235
$2t_{1u}$	− 0.373	$2t_{1u}$	− 0.371	− 0.377	− 0.369
$1e_g$	− 0.410	$1t_{1g}$	− 0.416	− 0.416	− 0.418
$1t_{1g}$	− 0.412	$1t_{2u}$	− 0.421	− 0.421	− 0.422
$1t_{2u}$	− 0.418	$1t_{1u}$	− 0.428	− 0.428	− 0.428
$1t_{1u}$	− 0.434	$1e_g$	− 0.430	− 0.436	− 0.432
$1t_{2g}$	− 0.438	$1t_{2g}$	− 0.436	− 0.436	− 0.435
$1a_{1g}$	− 0.457	$1a_{1g}$	− 0.448	− 0.458	− 0.441

[a] IGLO-III basis on C and O. [b] Quasirelativistic metal ECP at quasirelativistically optimized structure. [c] Nonrelativistic metal ECP at nonrelativistically optimized structure.

the shielding tensors increase or decrease from $Cr(CO)_6$ to $Mo(CO)_6$ or $W(CO)_6$, while the corresponding $\varepsilon_k - \varepsilon_a$ also decreases or increases in the same direction. In these cases it seems that r_N^{-3} rather than $\Delta\varepsilon$ controls the magnitude of these contributions to Equation (1). The only useful correlation is due to the energy of the $1e_g$ MO. It is considerably stabilized in $Mo(CO)_6$ and $W(CO)_6$ compared to $Cr(CO)_6$, and its antibonding combination, $2e_g^*$, is correspondingly destabilized, in line with stronger σ bonding (see Table 4). Indeed, the contributions to σ_{av} from excitations out of $1e_g$ decrease in absolute value down the group (they are -94.4, -89.7, and -84.8 ppm for $Cr(CO)_6$, $Mo(CO)_6$, and $W(CO)_6$, respectively). However, the contributions from $1t_{1u}$ also decrease from $Cr(CO)_6$ to $Mo(CO)_6$, without a corresponding change in orbital energies. We find that a breakdown in terms of localized molecular orbitals, as carried out in the next section, is more amenable to intuitive rationalizations. We will also postpone the discussion of the differences between free and metal-bound CO to the next section.

E. LMO Decomposition and Interpretation of Shielding Tensors: As we employ the IGLO algorithm[6] for the determination of the gauge origin of the vector potential, we can obtain additional information on the mechanism of chemical shifts and chemical bonding by breaking the shielding tensor elements down into contributions from localized molecular orbitals (LMOs). This type of analysis has been shown to be extremely informative by Kutzelnigg and co-workers.[6] Thus, the IGLO algorithm gives us a distinct advantage in the interpretation of results, compared to other choices of gauge origin.

The LMO analysis of chemical shielding for the CO molecule has been carried out in detail previously, and the following general picture for the shielding has emerged[6] (cf. Tables 5 and 6): The isotropic, diamagnetic shielding of the carbon nucleus by the carbon 1s orbital is counteracted by paramagnetic contributions from the valence LMOs, that is, the lone pairs on carbon and oxygen as well as the C–O triple bond, to $\sigma_\perp$. The largest of these deshielding contributions is due to the carbon lone pair, followed by the oxygen lone pair, and the C≡O bonding LMOs (only the sum of the C≡O contributions is given in Tables 5 and 6). The contributions to $\sigma_\parallel$ are all diamagnetic;[6, 25] this results in the known large anisotropy (ca. 400 ppm) of the shielding tensor. The deshielding contributions to $\sigma_\perp$ dominate the isotropic shift, with the correspondingly low absolute shielding. One may envision a "rotation" of the lone pair and bonding orbitals onto the C–O π-antibonding orbitals by the magnetic vector potential, leading to the large paramagnetic contributions to $\sigma_\perp$.[6] A similar mechanism is responsible for the highly anisotropic oxygen shielding tensor. In this case, the oxygen lone pair contributions to $\sigma_\perp$ exceed those from the carbon lone pair (Table 6).

We now can examine how this picture changes when the CO molecule is bound to a Group 6 metal fragment (Tables 5 and 6, Figures 2 and 3). As expected, the diamagnetic contributions from the respective 1s orbitals remain unchanged. Looking first at the carbon shielding tensor (Table 5, Fig. 2), we find that the involvement of the carbon lone pair in M–C σ bonding increases the deshielding contributions from this LMO to $\sigma_\perp$ considerably (the contributions to $\sigma_\parallel$ are almost unchanged). This may be due to changes both in $\Delta\varepsilon$ (see Eq. (1)) and in r_N^{-3} (plots of electron localization functions indicate the M–C bond to be more spacially confined around the carbon atom than the carbon lone pair in free CO[27]). However, a decrease in the deshielding terms involving the oxygen lone pair and the triple-

Table 5. Breakdown of the carbon shielding tensors in terms of LMO contributions [a].

LMO	CO			$Cr(CO)_6$			$Mo(CO)_6$			$W(CO)_6$ [e]		
	$\sigma_\perp$	$\sigma_\parallel$	σ_{av}	$\sigma_\perp$	$\sigma_\parallel$	σ_{av}	$\sigma_\perp$	$\sigma_\parallel$	σ_{av}	$\sigma_\perp$	$\sigma_\parallel$	σ_{av}
1s(C)	200.1	200.1	200.1	200.1	200.1	200.1	200.1	200.1	200.1	200.1	200.1	200.1
LP(C)/Bd(M–C)	−139.8	27.3	−84.1	−194.5	23.7	−121.8	−182.6	23.9	−113.8	−177.6	23.8	−110.5
LP(O)	−65.5	3.2	−42.6	−57.3	3.4	−37.0	−56.8	3.3	−36.7	−55.4	3.4	−35.9
3 × Bd(C≡O)	−122.8	41.7	−68.0	−98.7	49.3	−49.4	−100.0	48.7	−50.3	−97.0	50.4	−47.9
$\Sigma(n-1)$p(M) [b]				−12.0	−5.9	−9.9	−11.1	−1.6	−7.9	−11.8	−1.2	−8.2
$\Sigma(n-1)$d(M) [b]				−17.2	−7.7	−13.9	−17.8	−7.0	−13.9	−14.7	−7.7	−12.7
Σ [c]	−128.0	272.3	5.4	−179.5	263.0	−31.9	−167.4	267.5	−22.4	−156.4	268.7	−15.1
Total [d]	−127.9	272.6	5.6	−177.5	259.6	−31.8	−166.2	265.8	−22.2	−155.7	266.5	−14.9

[a] Absolute shieldings in ppm. Only LMOs with at least one individual contribution >3 ppm have been included. IGLO-III basis on C and O. LP = lone pair, Bd = bond. [b] Sums of contributions from metal $(n-1)$p-AO (semicore) and $(n-1)$d-AO-like LMOs. [c] Sum of all listed contributions. [d] Sum of all contributions. [e] At experimental solid-state structure (Table 1).

Table 6. Breakdown of the oxygen shielding tensors in terms of LMO contributions [a].

LMO	CO			$Cr(CO)_6$			$Mo(CO)_6$			$W(CO)_6$ [e]		
	$\sigma_\perp$	$\sigma_\parallel$	σ_{av}	$\sigma_\perp$	$\sigma_\parallel$	σ_{av}	$\sigma_\perp$	$\sigma_\parallel$	σ_{av}	$\sigma_\perp$	$\sigma_\parallel$	σ_{av}
1s(O)	270.2	270.2	270.2	270.2	270.2	270.2	270.2	270.2	270.2	270.2	270.2	270.2
LP(C)/Bd(M–C)	−115.4	4.1	−75.6	−120.5	3.1	−79.3	−115.1	3.2	−75.7	−107.3	3.2	−70.5
LP(O)	−217.7	34.5	−133.6	−178.8	35.0	−107.5	−176.1	34.9	−105.8	−168.4	34.9	−100.6
3 × Bd(C≡O)	−218.8	102.1	−111.9	−256.2	72.8	−146.6	−243.6	73.7	−138.6	−234.4	67.7	−133.7
$\Sigma(n-1)$p(M) [b]				−12.0	−8.0	−10.6	−9.9	−5.7	−8.6	−8.4	−6.3	−7.9
$\Sigma(n-1)$d(M) [b]				−14.8	−9.5	−13.1	−16.8	−12.2	−15.3	−14.2	−14.0	−13.8
Σ [c]	−281.7	410.9	−50.9	−312.0	363.7	−86.8	−291.8	363.1	−73.8	−262.8	355.7	−56.3
Total [d]	−281.7	411.2	−50.7	−311.3	359.0	−87.9	−293.4	363.1	−73.8	−260.3	351.7	−56.3

[a] Absolute shieldings in ppm. Only LMOs with at least one individual contribution >5 ppm have been included. IGLO-III basis on C and O. [b] Sums of contributions from metal $(n-1)$p-AO (semicore) and $(n-1)$d-AO-like LMOs . [c] Sum of all listed contributions. [d] Sum of all contributions. [e] At experimental solid-state structure (Table 1).

0947-6539/96/0201-0028 $ 10.00+.25/0 Chem. Eur. J. 1996, 2, No. 1

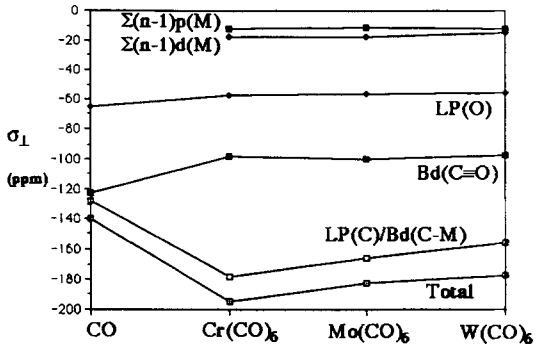

Fig. 2. Major LMO contributions to $\sigma_\perp(^{13}C)$. See Table 5. The contribution from the carbon 1s orbital (+ 200.1 ppm) has been omitted.

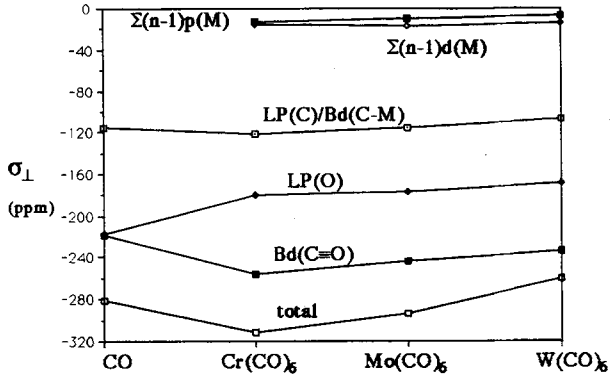

Fig. 3. Major LMO contributions to $\sigma_\perp(^{17}O)$. See Table 6. The contribution from the oxygen 1s orbital (+ 270.2 ppm) has been omitted.

bond LMOs partially compensates for this effect of the M–C σ-bonding LMO. The presence of additional deshielding contributions from metal $(n-1)$d- and $(n-1)$p-like LMOs (ca. −20 ppm to σ_{av}, summed up in $\sum(n-1)$d(M) and $\sum(n-1)$p(M) in Table 5) has to be included to account for the high-frequency shift of the carbon resonance upon binding of the CO ligand to the metal fragment.

The magnitude of the paramagnetic contributions from the M–C σ bond to $\sigma_\perp$ of the carbon nucleus decreases upon going from $Cr(CO)_6$ to $W(CO)_6$, exactly parallel to the corresponding absolute shielding tensor elements (Fig. 2). The deshielding contributions from the other valence LMOs to $\sigma_\perp$ and all contributions to $\sigma_\parallel$ (except for a slightly larger value of the metal d-orbital contribution for $Cr(CO)_6$) are roughly constant along this series. This includes the contributions from occupied metal d orbitals. Our results thus confirm previous arguments,[28] based on simple semiempirical considerations, that d–d excitations cannot account for the periodic trend. The increase in shielding down the group is largely due to the decrease in the absolute values of the paramagnetic contributions from the metal–carbon σ bond to $\sigma_\perp$ (Fig. 2).

A much more complicated situation pertains to the oxygen shielding tensor (Table 6, Fig. 3). Neither the deshielding upon binding of CO to a Group 6 metal center nor the small increase in shielding from $Cr(CO)_6$ to $W(CO)_6$ may be attributed to just one dominant term. While the contributions from the oxygen lone pair to $\sigma_\perp$ are less deshielding in the complexes than in the free ligand, all other terms become somewhat more deshielding (including the contributions from metal $(n-1)$d and $(n-1)$p orbitals, which are absent for free CO). All terms become slightly less paramagnetic down Group 6, but no contribution can be singled out (Fig. 3).

Conclusions

Our combined ECP/DFT[3] approach has allowed the accurate calculation and a detailed interpretation of NMR ^{13}C and ^{17}O chemical shift tensors for the Group 6 hexacarbonyl complexes. As the method used is computationally inexpensive, ligand NMR shielding tensors in considerably larger complexes or clusters are now accessible to detailed investigation. We are presently carrying out work along these lines.[27]

The break down of the shielding-tensor elements, in terms of both localized molecular orbital (LMO) and canonical MO contributions, has improved our understanding of the mechanism of ligand chemical shielding in transition-metal carbonyl complexes. The changes in carbon shielding upon binding of CO to a metal fragment are accompanied by changes in a variety of orbital contributions, among them the presence of excitations out of occupied metal d orbitals and of semi-core $(n-1)$p orbitals. The trend to more shielding from $Cr(CO)_6$ to $Mo(CO)_6$ to $W(CO)_6$ is due to decreased paramagnetic contributions mainly from C–M σ-bonding orbitals, involving excitations into C≡O antibonding orbitals. A relation to d–π* back-bonding is at best indirect and could arise from the synergistic interplay of σ and π bonding.[29]

Scalar relativistic effects are moderate but important for the differences between the molybdenum and tungsten complexes. Probably, spin–orbit coupling needs to be included to obtain an even more accurate difference between the carbon shieldings for $W(CO)_6$ and $Mo(CO)_6$. We expect that the present results may be generalized to other comparisons of ligand chemical shielding tensors for typical terminal carbonyl ligands. More unusual terminal, and bridging carbonyl ligands, as well as other ligands in transition-metal complexes are presently under investigation.[27]

Acknowledgements: Part of this work was carried out during a one-year stay of M. K. in Montréal, kindly sponsored by a Canada Scholarship of the NSERC. M. K. is also grateful to the DFG for a "Habilitationsstipendium" and to Prof. H. G. von Schnering (Max-Planck-Institut, Stuttgart) for his continuing support and for providing computational resources. Further computer resources were provided by the Services Informatiques de l'Université de Montréal. Financial support from NSERC and from the Slovak Grant Agency for Science (grant no. 1172/94) is gratefully acknowledged. This work has also benefitted from the earlier Alexander von Humboldt Fellowship of VGM at the Ruhr-Universität Bochum. We thank an unknown referee for helpful suggestions.

Received: April 5, 1995 [F115]

[1] For recent overviews, cf.: *Nuclear Magnetic Shieldings and Molecular Structure* (Ed. J. A. Tossel) Kluwer Academic Publishers, Dordrecht **1993**; D. B. Chesnut in *Annual Reports on NMR Spectroscopy*, Vol. 29, Academic Press, London **1994**, pp. 71–122.

[2] Cf., e.g.: a) D. A. Brown, J. P. Chester, N. J. Fitzpatrick, I. J. King *Inorg. Chem.* **1977**, *16*, 24. b) J. Evans, J. R. Norton, *ibid.* **1974**, *13*, 3042. c) *^{13}C NMR Data for Organometallic Compounds*, B. E. Mann, B. F. Taylor, Academic Press, London **1981**.

[3] M. Kaupp, V. G. Malkin, O. L. Malkina, D. R. Salahub, *Chem. Phys. Lett.* **1995**, *235*, 382.

[4] a) V. G. Malkin, O. L. Malkina, M. E. Casida, D. R. Salahub *J. Am. Chem. Soc.* **1994**, *116*, 5898. b) V. G. Malkin, O. L. Malkina, L. A. Eriksson, D. R. Salahub in *Modern Density Functional Theory: A Tool for Chemistry; Theoretical and Computational Chemistry*, Vol. 2 (Eds.: J. M. Seminario, P. Politzer) Elsevier, Amsterdam **1995**.

[5] M. Kaupp, V. G. Malkin, O. L. Malkina, D. R. Salahub, *J. Am. Chem. Soc.* **1995**, *117*, 1851; *ibid.* **1995**, *117*, 8492.

[6] W. Kutzelnigg, U. Fleischer, M. Schindler in *NMR—Basic Principles and Progress*, Vol. 23, Springer, Heidelberg **1990**, p. 165.

[7] G. E. Hawkes, K. D. Sales, S. Aime, R. Gobetto, L.-Y. Lian *Inorg. Chem.* **1991**, *30*, 1489.

[8] J. W. Gleeson, R. W. Vaughan, *J. Chem. Phys.* **1983**, *78*, 5384.

[9] Cf., e.g.: a) H. Mahnke, R. K. Sheline, H. W. Spiess, *J. Chem. Phys.* **1974**, *61*, 55. b) T. H. Walter, L. Reven, E. Oldfield, *J. Phys. Chem.* **1989**, *93*, 1320.

c) T. H. Walter, A. Thompson, M. Keniry, S. Shinoda, T. L. Brown, H. S. Gutowsky, E. Oldfield, *J. Am. Chem. Soc.* **1988**, *110*, 1065, and references therein.
[10] E. Oldfield, M. A. Keniry, S. Shinoda, S. Schramm, T. L. Brown, H. S. Gutowsky, *J. Chem. Soc. Chem. Commun.* **1985**, 791.
[11] The metal shielding tensor in $Mo(CO)_6$ has been calculated at the Hartree–Fock level (J. E. Combariza, M. Barfield, J. H. Enemark, J. C. Facelli, *J. Am. Chem. Soc.* **1989**, *111*, 7619).
[12] D. R. Salahub, R. Fournier, P. Mlynarski, I. Papai, A. St-Amant, J. Ushio in *Density Functional Methods in Chemistry* (Eds.: J. K. Labanowski, J. W. Andzelm) Springer, New York **1991**, p. 77. A. St-Amant, D. R. Salahub, *Chem. Phys. Lett.* **1990**, 169, 387. A. St-Amant, Thesis, Université de Montréal, **1992**.
[13] a) M. Dolg, U. Wedig, H. Stoll, H. Preuss, *J. Chem. Phys.* **1987**, *86*, 866. b) D. Andrae, U. Häussermann, M. Dolg, H. Stoll, H. Preuss, *Theor. Chim. Acta* **1990**, *77*, 123.
[14] The procedure follows: M. Pelissier, N. Komiha, J. Daudey, *J. Comput. Chem.* **1988**, *9*, 298.
[15] M. Kaupp, H.-J. Flad, A. Köster, H. Stoll, D. R. Salahub, unpublished results.
[16] C. van Wüllen, *Int. J. Quant. Chem.*, in press.
[17] J. P. Perdew, Y. Wang, *Phys. Rev. B* **1992**, *45*, 13244; J. P. Perdew in *Electronic Structure of Solids* (Eds.: P. Ziesche, H. Eischrig) Akademie Verlag, Berlin **1991**; J. P. Perdew, J. A. Chevary, S. H. Vosko, K. A. Jackson, M. R. Pederson, D. J. Singh, C. Fiolhais, *Phys. Rev. B* **1992**, *46*, 6671.
[18] J. M. Foster, S. F. Boys, *Rev. Mod. Phys.* **1963**, *35*, 457.
[19] A. Bergner, M. Dolg, W. Küchle, H. Stoll, H. Preuss, *Mol. Phys.* **1993**, *80*, 1431.
[20] A. D. Becke, *Phys. Rev. A* **1988**, *38*, 3098; J. P. Perdew, *Phys. Rev. B* **1986**, *33*, 8822.
[21] J. Li, G. Schreckenbach, T. Ziegler, *J. Phys. Chem.* **1994**, *98*, 4838.
[22] Cf., e.g.: a) W. Kutzelnigg, C. v. Wüllen, U. Fleischer, R. Franke, T. v. Mourik in ref. [1], p. 141; b) S. P. A. Sauer, I. Paidarova, J. Oddershede, *Mol. Phys.* **1994**, *81*, 87; c) J. Gauss, *J. Chem. Phys.* **1993**, *99*, 3629; d) K. Ruud, T. Helgaker, R. Kobayashi, P. Jorgensen, K. L. Bak, H. J. Aa. Jensen, *ibid.* **1994**, *100*, 8178; e) H. Fukui, T. Baba, H. Matsuda, K. Miura, *ibid.* **1994**, *100*, 6608.
[23] a) J. Gauss, *Chem. Phys. Lett.* **1994**, *229*, 198. b) J. Gauss, J. F. Stanton, *J. Chem. Phys.* **1995**, *103*, 3561.
[24] A. A. V. Gibson, T. A. Scott, E. Fukushima, *J. Magn. Res.* **1977**, *27*, 29.
[25] A. J. Beeler, A. M. Orendt, D. M. Grant, P. W. Cutts, J. Michl, K. W. Zilm, J. W. Downing, J. C. Facelli, M. S. Schindler, W. Kutzelnigg, *J. Am. Chem. Soc.* **1984**, *106*, 7672.
[26] A. K. Jameson, C. J. Jameson, *Chem. Phys. Lett.* **1987**, *134*, 461.
[27] For example: M. Kaupp, *Chem. Eur. J.*, in press.
[28] D. Cozak, I. S. Butler, *Can. J. Chem.* **1977**, *55*, 4056.
[29] J. P. Hickey, J. R. Wilkinson, L. J. Todd, *J. Organomet. Chem.* **1979**, *179*, 159.
[30] R. E. Wasylishen, S. Mooibroek, J. B. Macdonald, *J. Chem. Phys.* **1984**, *81*, 1057.

0947-6539/96/0201-0030 $ 10.00+.25/0